

Dynamic MBSFN Beam Area Formation in 6G Multi-Beam Non-Terrestrial Networks

Federica Rinaldi, *Member, IEEE*, Angelo Tropeano, Sara Pizzi, Antonella Molinaro, *Senior Member, IEEE*, and Giuseppe Araniti, *Senior Member, IEEE*.

Abstract—Providing innovative services and ensuring ubiquitous, ultra-high density, extreme data-rate, and very-low latency communications are essential for future Sixth-Generation (6G) systems, where the importance of Non-Terrestrial Networks (NTNs) will incredibly rise. However, the management of both capacity and radio spectrum remains one of the main challenges, when a huge number of devices requires access to dissimilar broadcast services at the same time. To cope with these issues, traditional single-beam satellite systems can be replaced with Very-High Throughput Satellite (VHTS), where multi-beam transmissions increase the capacity, improve the spectrum utilization while limiting inter-beam interference. In this paper, we propose a Dynamic MBSFN (Multicast/Broadcast Single Frequency Network) Beam Area Formation (D-MBAF) algorithm that dynamically groups beams into dedicated MBSFN Beam Areas (MBAs) to increase the Aggregate Data Rate (ADR) of the multi-beam NTN system and deliver a given video content to all the interested NTN terminals. D-MBAF leverages multicast subgrouping by clustering the NTN terminals into different MBAs that are simultaneously served with different data rates. Furthermore, the D-MBAF algorithm delivers the video content in different flows: the base layer with lower resolution and a set of enhancement layers with higher resolutions. Radio resources are efficiently allocated to avoid interference among the beams belonging to different MBAs. A simulation campaign is carried out under different scenarios to assess the effectiveness of the proposed D-MBAF algorithm in terms of mean throughput, ADR, resource block utilization, and number of sent layers. Obtained results confirm that the D-MBAF algorithm outperforms the Single-Frequency Multi-Beam Transmission and the multi-layer video delivery schemes used as benchmarks.

Index Terms—Non-Terrestrial Networks, Satellite Communication, 6G, New Radio, Multicast Subgrouping, MBSFN.

I. INTRODUCTION

IN recent years, the interest in Non-Terrestrial Networks (NTNs) [1] has increased and will continue to rise. Indeed, telecommunication operators and the scientific research community investigate new cutting-edge solutions to make the NTN an effective alternative/complement to the terrestrial network. Owing to the large footprint size, NTNs can deliver services anytime and anywhere, even on-board cruises, high-speed trains, and airplanes by providing coverage in places where installing terrestrial networks is not economically convenient or even impossible due to the morphology of the territory. Moreover, NTNs can offer service continuity

and ubiquity while achieving network scalability, by providing multicast/broadcast data delivery to NTN terminals and network edges, and can guarantee network resilience by integration with the terrestrial networks [2]. NTNs can be significantly advantageous to deliver broadband services even in remote places.

To support broadband connectivity, the traditional single-beam satellites must be replaced by multi-beam satellites. Specifically, High Throughput Satellite (HTS) and Very-HTS (VHTS) systems are good candidates to deliver the bandwidth-hungry and very high-data rate services (typically video-based) that will characterize the future Sixth-Generation (6G) network. Indeed, video services will be responsible for the growth of mobile data traffic, representing 77% of such growth expected to reach 237EB per month by 2026 [3]. New emerging business cases will be supported by the 6G technology, most of which include video-based applications, such as Holographic Type Communications (i.e., entertainment and teleconferencing services, telesurgery, telepresence, and others) with great impact on our life. Given the ever increasing number of requests to access high-quality video content expected over the coming years, there will be the need to manage a huge amount of data traffic from uncompressed video signals.

In the described context, the efficient management of the system capacity and the radio spectrum is especially challenged by the massive number of end-devices simultaneously demanding dissimilar broadcast services. To cope with this issue, HTS/VHTS-based NTNs promise an increase in the capacity and an improvement in the spectrum utilization thanks to multi-beam transmissions and limited inter-beam interference by exploitation of color-based frequency reuse schemes, where the beams share different frequency sets on the basis of the considered frequency reuse factor (FRF) [4].

In the past literature, several methods have tried to limit the inter-beam interference in HTS/VHTS-based NTNs. In particular, the Single-Frequency Multi-Beam Transmission (SF-MBT) [5] proposes the grouping of adjacent beams into a single Multicast/Broadcast Single Frequency Network (MBSFN) Beam Area (MBA) to perform time-synchronized transmissions of the same content over the same radio resources. Despite the SF-MBT algorithm improves the system capacity by reusing the same set of radio resources in all the beams of a MBA, its parameters selection is affected by the NTN terminal with the poorest channel conditions, at the cost of increasing the dissatisfaction of the NTN terminals with a better channel quality. Therefore, new solutions are needed that consider the

F. Rinaldi, A. Tropeano, S. Pizzi, A. Molinaro, and G. Araniti are with the DIIES Department, University Mediterranea of Reggio Calabria, Via Graziella Loc. Feo di Vito, 89100 Reggio Calabria, Italy, and with CNIT. A. Molinaro is also with Paris-Saclay University. (e-mail: federica.rinaldi@unirc.it, angelo.tropeano@unirc.it, sara.pizzi@unirc.it, antonella.molinaro@unirc.it, araniti@unirc.it).

heterogeneous channel qualities of different NTN terminals and, accordingly, group them in the appropriate MBA.

In this paper, we propose a Dynamic MBSFN Beam Area Formation (D-MBAF) algorithm that dynamically groups beams into dedicated MBAs to increase the Aggregate Data Rate (ADR) of the multi-beam NTN system and to deliver the video content to all the NTN terminals which are interested in receiving it. D-MBAF leverages multicast subgrouping by clustering the NTN terminals into different subsets based on their Channel State Information (CSI), and simultaneously serving them at different data rates.

Specifically, D-MBAF creates several MBAs according to channel feedbacks from NTN terminals, considering the heterogeneity of collected CSI and the NTN terminal distribution across the beams of the multi-beam NTN system. Furthermore, D-MBAF supports the video content delivery in more flows: the base layer with lower resolution (i.e., High-Definition or HD) and a set of enhancement layers with higher resolutions (i.e., Full HD or FHD, 4K, and 8K). Each created MBA, consisting of adjacent beams, delivers a certain video layer with a given Modulation and Coding Scheme (MCS), by exploiting a portion of the available radio resources to avoid interference among the beams belonging to different MBAs (i.e., inter-MBA interference). All NTN terminals receive the base video layer, while NTN terminals with better channel conditions receive also one or more enhancement video layers according to their experienced CSI.

It is worth noting that D-MBAF avoids inter-beam interference and inter-MBA interference. Avoiding inter-beam interference is possible owing to the Single Frequency Network (SFN) transmission. Indeed, by definition, all the cells (in our case, all the beams) within a SFN (in our case, within an MBA) are synchronized in time to deliver the same content, within a given cyclic prefix (CP) interval, by exploiting the same radio resources. In such a way, the different signals arriving within the CP are combined, thus acting as constructive interference and improving the signal perceived by the NTN terminals with worse channel conditions. Avoiding inter-MBA interference is possible owing to the D-MBAF's Radio Resource Management (RRM) procedure. In particular, the algorithm splits radio resources among each MBA according to the minimum data rate required by each service layer (i.e., base or enhancements). In such a way, the NTN terminals receive base and enhancement layers from the base MBA and enhancement MBAs, respectively, which exploit different sets of radio resources, thus avoiding interfering with each other.

The list of main acronyms and abbreviations used in this paper is shown in Table I.

The remainder of this paper is organized as follows. In Section II, we review the state of the art in the related field and illustrate our main contributions. In Section III, we describe the scenario, define the reference system and channel models. The proposed D-MBAF algorithm and its computational complexity are presented in Section IV. An extensive analysis of the performance results is provided in Section V. Finally, conclusions are drawn in Section VI.

TABLE I: Abbreviations and acronyms

5G	Fifth-Generation
5GC	5G Core Network
6G	Sixth-Generation
ADR	Aggregate Data Rate
AMC	Adaptive Modulation and Coding
CP	Cyclic Prefix
CP-OFDM	Cyclic Prefix – Orthogonal Frequency-Division Multiplexing
CQI	Channel Quality Indicator
CSI	Channel State Information
DFT-s-OFDM	Discrete Fourier Transform – spread – OFDM
D-MBAF	Dynamic MBSFN Beam Area Formation
eMBB	enhanced Mobile Broadband
eMBMS	evolved-Multimedia Broadcast/Multicast Service
FHD	Full High Definition
FRF	Frequency Reuse Factor
gNB	gNodeB, 5G Base Station
GEO	Geostationary Equatorial Orbit
GEO-gNB	GEO-sat component on the ground
GEO-sat	GEO satellite with transparent payload
HD	High Definition
HEVC	High Efficiency Video Coding
HTS	High Throughput Satellite
LMS	Land-Mobile Satellite
LoS	Line-of-Sight
μ	Numerology
MBA	MBSFN Beam Area
MBSFN	eMBMS over Single Frequency Network
MCS	Modulation and Coding Scheme
MS	Multicast Subgrouping
N6	Air interface between the 5G Core Network and the service provider
NG	Next-Generation air interface between the gNodeB and the 5G Core Network
NG-RAN	Next-Generation Radio Access Network
NTN	Non-Terrestrial Network
NTN-GW	Non-Terrestrial Network Gateway
NR	New Radio
NR-Uu	New Radio between Universal Terrestrial Radio Access Network (UTRAN) and User Equipment (UE)
OFDM	Orthogonal Frequency-Division Multiplexing
RB	Resource Block
RRM	Radio Resource Management
RRU	Remote Radio Unit
RTD	Round Trip Delay
SBA	Synchronization Beam Area
SCS	Sub-Carrier Spacing
SF-MBT	Single-Frequency Multi-Beam Transmission
TTI	Transmission Time Interval
VHTS	Very High Throughput Satellite
VR	Virtual Reality
VSAT	Very Small Aperture Terminal

II. STATE-OF-THE-ART REVIEW

Adaptive Modulation and Coding (AMC) is one of the most investigated issues related to multicast transmissions, where the link adaptation procedure is performed to set the transmission parameters on a per-group basis. Indeed, a content is delivered by adopting the most robust modulation (i.e., the lowest MCS) supported by all target users to be correctly received and decoded. The main AMC schemes proposed in the literature for single beam-based satellite systems are described below.

The Conventional Multicast Scheme adapts the transmission parameters to those users experiencing the worst channel conditions, thus guaranteeing fairness among users but suffering from low spectral efficiency [6]. The Multicast Link

Adaptation, or opportunistic scheme, envisages that a subset of the multicast group is being served to optimize a certain objective function [7]. In Multicast Subgrouping (MS), the multicast group is split into subgroups, wherein users perceive similar channel conditions and are served [8]. In [9], the Multicast Subgrouping-Maximum Satisfaction Index scheme optimizes the user satisfaction indices by guaranteeing the throughput-fairness trade-off. In [10], MS is combined with the Application-Layer Joint Coding technique [11] to offer high throughput and compensate for packet losses, thus improving the perceived video quality of satellite multicast transmissions.

Besides enabling multicast transmission to improve system capacity and spectrum utilization, satellite systems based on multiple beams (i.e., HTS and VHTS) represent the evolution of the traditional Fixed Satellite System based on a single beam footprint. Multi-beam transmissions leverage the principle of frequency reuse to let nearby beams exploit different bandwidths to limit inter-beam interference, which is caused when all the beams reuse the same frequency thus limiting the performance of HTS (or VHTS) systems. To overcome the issue of inter-beam interference, several solutions on precoding, RRM, and beam area formation have been proposed in past literature.

Pre-coding techniques mitigate the interference generated by side lobes in beam radiation patterns at the beam edges. In [12], an optimal solution addresses the linear pre-coding problem. In [13], multicast multigroup pre-coding techniques and user clustering methods have been overviewed for multi-beam satellite communications. In [14], an optimization frame-based pre-coding problem has been formulated for throughput maximization in a satellite system. In [15], the problem of multicast multigroup transmission has been investigated for frame-based multi-beam satellite systems and a low complexity pre-coder has been proposed for robust power minimization by considering the CSI at the transmitter (CSIT) for user clustering. In [16], a low complexity two-stage pre-coding scheme has overcome the effect related to imperfect CSIT due to long propagation delays. In [4], to be simultaneously served in the same frame, users have been grouped into a cluster according to two k -means based clustering approaches. In [17], a novel mathematical framework addresses the problem of user clustering for throughput maximization. Differently from the above-cited works, where the focus was on multicast multigroup pre-coding or user clustering, in [18] the impact of the system scheduler has been analyzed on multicast pre-coding, and a geographical scheduling algorithm has been developed to improve the performance of multicast and unicast pre-coding against random scheduling.

Appropriate RRM policies can also mitigate inter-beam interference. In [19] a novel resource allocation scheme, considering user locations and different radio propagation conditions, has been formulated for multi-beam satellite systems. Since a varying channel hurts the performance of a multi-beam satellite system, a new method for channel estimation and a novel detection technique have been proposed in [20]. In [21] a new dynamic bandwidth allocation scheme has achieved the trade-off between capacity and fairness in scenarios with uniform signal attenuation across beams and different traffic

demands. In [22] a dynamic channel allocation algorithm has been proposed and an optimization problem has been formulated by considering deep reinforcement learning techniques for the minimization of the service blocking probability in multi-beam satellite systems. In [23] power and bandwidth allocation has been solved with a genetic algorithm considering the propagation effects, interference among beams, and atmospheric attenuation. In [24] the constructed mathematical model and the derived power allocation scheme have achieved the trade-off between transmit power and beam directivity and increased the flexibility of managing different traffic demands.

Recently, the MBA has been defined as another method to mitigate inter-beam interference. The concept of MBA extends the idea of MBSFN Area involving the cells of terrestrial systems to the beams of satellite networks. In cellular systems, an MBSFN Area is conceived as a set of adjacent cells that reuse the same radio resources to simultaneously deliver a certain content. The heuristic approach, proposed in [25] to cluster cells into MBSFN Areas according to users interests, considers the generation of multi-content MBSFN areas and maximization of the system throughput by combining unicast and multicast transmissions. The algorithm proposed in [26] maximizes the ADR by dynamically generating both Overlapping MBSFN areas, delivering more than one video layer with different resolutions to improve the Quality of Service (QoS) of users with good channel conditions, and Disjoint MBSFN areas, delivering the demanded contents with a basic resolution by selecting the most robust modulation supported by all users in the area. Differently from [26], the algorithm proposed in [27] adds device-to-device (D2D) communications as a third mode to receive the content; hence, users may receive the service through either MBSFN, or D2D, or unicast transmissions. In [28], a graph-based greedy algorithm has been proposed to configure MBSFN areas in a flexible manner and solve the problem of area partitioning.

In analogy to cellular systems, in satellite networks the MBA exploits simultaneous MBSFN transmissions among time-synchronized beams to mitigate the interference between the NTN terminals at the beam edges. In [5], the Single-Frequency Multi-Beam Transmission (SF-MBT) scheme, introduced to overcome the issues related to color-based frequency reuse techniques [29], considers that adjacent beams synchronized in time and belonging to the same satellite simultaneously deliver a certain content over the same radio resources thus improving the signal strength at the NTN receivers, since multiple signal waveforms arrive within the CP interval and constructively interfere.

CONTRIBUTIONS: To the best of our knowledge, the problem of MBSFN Beam Area formation has not been investigated for multi-beam satellite communications. Therefore, the main contribution of this work is the design of a heuristic algorithm for dynamic MBA formation (D-MBAF), which improves the performance of multi-beam NTN systems expected for 6G. Specifically, D-MBAF leverages multicast subgrouping to increase the throughput of NTN terminals the High-Efficiency Video Coding (HEVC) and to improve the video quality. The D-MBAF algorithm (*i*) selects the best MBA configuration that increases the ADR as much

as possible, (ii) performs radio resource allocation among the created MBAs for efficient radio spectrum utilization, (iii) serves all the NTN terminals interested in the delivered content, and (iv) enhances the perceived video quality of NTN terminals experiencing good channel conditions.

III. SYSTEM MODEL

As depicted in Fig. 1, we consider a multi-beam NTN radio access network enabling multicast transmissions where the NTN platform is connected to the 5G Core Network (5GC) through the NTN Gateway and directly communicates with the NTN terminals via the NR-Uu radio interface.

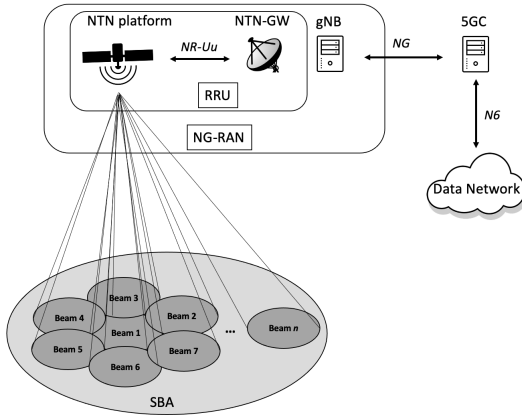


Fig. 1: Reference architecture for executing the D-MBAF algorithm over a multi-beam NTN system.

A. Scenario Description

A Geostationary Earth Orbit (GEO)-based HTS (GEO-sat) equipped with a transparent payload [1] operating in the Ka-band frequencies (i.e., 20 GHz) is considered as the reference NTN platform. The GEO-sat ground component is the GEO-gNB that is in charge of performing link adaptation procedures. Specifically, after receiving all the CSI feedbacks of the NTN terminals from the GEO-sat through the feeder link, the GEO-gNB selects transmission parameters by choosing the appropriate MCS for the delivery of a certain content to multiple recipients through the service link.

The time needed by a signal to travel from the NTN terminal to the NTN gateway and back (or vice versa) is known as Round Trip Delay (RTD). For a transparent payload-based GEO satellite, the RTD is 541.46 ms [1].

Since the 3GPP focuses on adapting the latest New Radio (NR) standard to support NTNs, we consider a 6G multi-beam NTN system based on the NR technology supporting multiple scalable Orthogonal Frequency Division Multiplexing (OFDM) numerologies ($\mu=0$ to 4). Each numerology is characterized by a value of Sub-Carrier Spacing ($SCS = 15kHz$ to $240kHz$), as specified in the following equation [2]:

$$SCS = 15kHz \times 2^\mu, \quad (1)$$

where μ is the numerology index. The NR modulation technique is CP-OFDM, which stands for OFDM with CP, for the

downlink (DL), whereas both CP-OFDM and Discrete Fourier Transform-spread-OFDM (DFT-s-OFDM) with CP are for the uplink (UL). NR transmissions in DL and UL directions are organized in frames. Each frame consists of subframes lasting 1 ms and having as many slots as given by the numerology.

The radio spectrum is managed in terms of Resource Blocks (RBs). One RB is defined by 12 consecutive and equally spaced sub-carriers. In this paper, we choose the numerology $\mu = 2$ with $SCS = 60kHz$, which is supported by NTN operating in Ka-band frequencies [1].

B. D-MBAF in a Nutshell

The proposed D-MBAF aims to (i) dynamically create dedicated MBAs, wherein the beams perform simultaneous MBSFN Beam transmissions of a demanded content with certain video quality, and (ii) efficiently allocate the radio resources in order to ensure the minimum data rate requested by a given video layer while providing a higher ADR in a multi-beam NTN system with respect to benchmark approaches. To achieve this goal, D-MBAF creates several MBAs, each consisting of adjacent beams that provide different video content resolutions. Specifically, the Base MBA groups all the beams to deliver the content with HD resolution to all NTN terminals. NTN terminals experiencing better channel conditions receive the content with an enhanced resolution by the beams inside Enhancement MBAs. D-MBAF considers three Enhancement MBAs, which transmit the content with FHD, 4K, and 8K video resolution, respectively.

Fig. 2 illustrates the D-MBAF behaviour with a flowchart. The working logic of the proposed algorithm is to group the beams belonging to the SBA of the HTS in several MBAs by taking into account both channel quality similarity and interests of NTN terminals. The generated MBAs may be either *independent*, if all the beams belong to a single MBA, or *overlapped* if at least one beam is shared among more MBAs. In the latter case, D-MBAF performs a proper radio resource allocation across the involved MBAs with the aim to avoid inter-beam interference, while ensuring the minimum required data rate to provide the content with the selected video resolution. Finally, D-MBAF enhances the system ADR by meeting the constraint of serving all NTN terminals interested in the content, and improving the video quality resolution of NTN terminals experiencing better channel conditions.

C. NR-enabled Multi-Beam NTN Model

We denote \mathcal{B} as the set of beams that cover a given area on Earth and belong to the Synchronization Beam Area (SBA). The SBA is the coverage area of a GEO-sat and may consist of one or more MBAs, each corresponding to two or more adjacent beam footprints. The beams of the same MBA perform an MBSFN Beam transmission by time-synchronizing the delivery of the same content to multiple recipients over the same radio resources.

Let \mathcal{M} be the set of all MBAs within an SBA given by:

$$\mathcal{M} = \mathcal{M}_{base} \cup \mathcal{M}_{enh}, \quad (2)$$

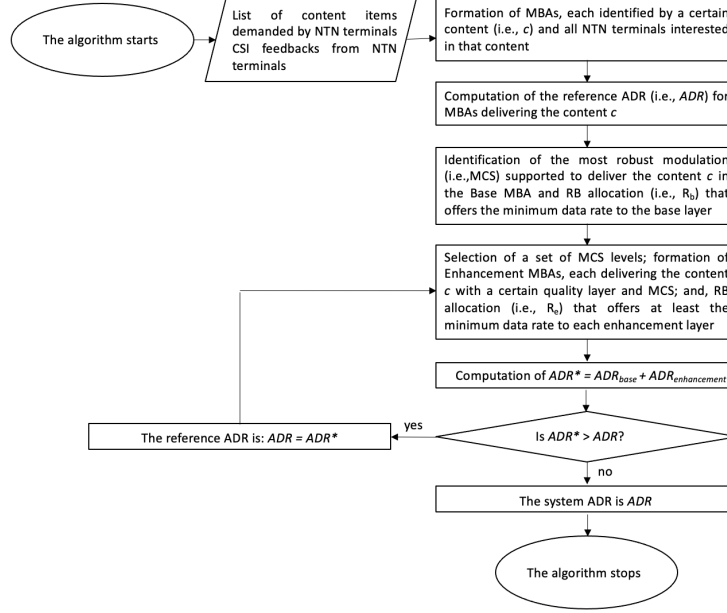


Fig. 2: Flowchart of the D-MBAF algorithm.

where \mathcal{M}_{base} is the set of all Base MBAs and \mathcal{M}_{enh} is the set of all Enhancement MBAs.

We denote \mathcal{C} as the set of all contents demanded by NTN terminals in the SBA. The set \mathcal{T} of all NTN terminals interested in the broadcasted video contents shall be served:

$$|\mathcal{T}| = \sum_{m_b \in \mathcal{M}_{base}} |\mathcal{T}_{m_b}|, \quad (3)$$

where the operator $|\cdot|$ represents the cardinal number of a certain set and \mathcal{T}_{m_b} is the set of NTN terminals receiving the Base Video Layer in the Base MBA m_b .

The set $\mathcal{T}_{m_e, l}$ is defined as the set of some or all the NTN terminals belonging to the set \mathcal{T}_{m_b} and receiving the l -th Enhancement Video Layer delivered in the Enhancement MBA m_e :

$$\mathcal{T}_{m_e, l} \subseteq \mathcal{T}_{m_b} \quad \forall l \in \mathcal{L} \quad (4)$$

Let R be the number of available radio resources (i.e., RBs). Let R_b and R_e be the number of RBs assigned to deliver the base layer and enhancement layers, respectively. We denote \mathcal{R}_e as the set of RBs intended for the Enhancement MBAs, and \mathcal{L} as the set of the Enhancement Video Layers.

The overall number of RBs to be allocated to the Base MBA and the three Enhancement MBAs shall not exceed the number of available RBs:

$$R_b + R_e \leq R. \quad (5)$$

The sum of RBs allocated to the Enhancement MBA m_e for delivering all the l -th Enhancement Video Layers shall not exceed the number of available RBs intended for transmitting the set of Enhancement Layers:

$$\sum_{l \in \mathcal{L}} |\mathcal{R}_{e_l, m_e}| \leq R_e, \quad \forall m_e \in \mathcal{M}_{enh}, \quad (6)$$

where the number of RBs allocated to deliver the l -th Enhancement Video Layer in the m_e -th Enhancement MBA is the ratio between the the minimum data rate required for the transmission of the l -th Enhancement Layer (i.e., DR_{e_l}) and the data rate achievable for the transmission of the l -th Enhancement Video Layer with the minimum MCS supported by the set $\mathcal{T}_{m_e, l}$ of NTN terminal belonging to the m_e -th Enhancement MBA (i.e., $DR_{MCS(\mathcal{T}_{m_e, l})}$), hence:

$$|\mathcal{R}_{e_l, m_e}| = \left\lceil \frac{DR_{e_l}}{DR_{MCS(\mathcal{T}_{m_e, l})}} \right\rceil, \quad \forall l \in \mathcal{L}, \forall m_e \in \mathcal{M}_{enh} \quad (7)$$

The purpose of the proposed D-MBAF algorithm is to create dedicated MBAs in a 6G multi-beam NTN system that meets the above constraints and performs link adaptation procedures by dynamically selecting the MCS level among those supported by the NTN terminals for the delivery of Base and Enhancement Video Layers. By referring to an SBA as the set \mathcal{M} of MBAs, the ADR is given by:

$$ADR = \sum_{m \in \mathcal{M}} ADR_m, \quad (8)$$

where the ADR of the NTN terminals receiving the content in the m -th MBA through the MBSFN Beam transmission is represented as:

$$ADR_m = ADR_{m_b} + ADR_{m_e}, \quad \forall m \in \mathcal{M}, \quad (9)$$

where

$$ADR_{m_b} = \sum_{t_b \in \mathcal{T}_{m_b}} DR_{MCS}(t_b) \times R_b, \quad \forall m_b \in \mathcal{M}_{base}, \quad (10)$$

is the ADR of NTN terminals receiving the Base Video Layer,

TABLE II: Loo model parameters for each environment for different orientations and sides of the road, Ka-band.

Environment	State 1: LOS			State 2: Moderate Shadowing			State 3: Deep Shadowing		
	α (dB)	Ψ (dB)	MP (dB)	α (dB)	Ψ (dB)	MP (dB)	α (dB)	Ψ (dB)	MP (dB)
Leaf Tree	-0.5	0.5	-25.0	-10.0	4.0	-25.0	-23.0	8.0	-25.0
Pine (or Needle) Tree	-0.4	0.5	-25.0	-10.0	4.0	-25.0	-29.0	3.0	-25.0
Tree Alley	0.0	0.5	-25.0	-10.0	3.0	-25.0	-21.0	4.0	-25.0
Suburban	0.0	0.5	-25.0	-9.0	3.0	-25.0	-21.0	4.0	-25.0
Urban	0.0	0.5	-25.0	-11.0	4.0	-25.0	-28.0	8.0	-25.0

$$ADR_{m_e} = \sum_{l \in \mathcal{L}} \sum_{t_e \in \mathcal{T}_{m_e, l}} DR_{MCS}(t_e, l) \times R_{e, m_e}, \forall m_e \in \mathcal{M}_{enh}, \quad (11)$$

is the ADR of NTN terminals receiving Enhancement Video Layers.

By using a heuristic approach, the proposed RRM scheme performs an adequate allocation of radio resources (i.e., the set \mathcal{R}) in order to deliver base and enhancement layers so that to maximize the ADR, thus solving the following problem:

$$\arg \max_{\mathcal{R}} ADR, \quad (12)$$

subject to (2) - (9).

D. Channel Model

We represent the Land-Mobile Satellite (LMS) channel by following the Pèrez-Fontán model [30], where three propagation conditions (i.e., LOS, moderate shadowing, and deep shadowing) are described by a three-state first-order Markov chain. The Markov chain is defined by the transition probability matrix \mathbf{P} and the state probability vector \mathbf{w} . The signal amplitude variations of each state that are due to shadowing and multipath phenomena follow three different parameters (i.e., α , Ψ , MP) of the Loo probability density function [31].

TABLE III: Markov Chain Matrices \mathbf{P} and state probability vectors \mathbf{w} for each modeled environment at an elevation angle of 30° , orientation of 45° , satellite side of the road, Ka-band.

Environment	\mathbf{w}	\mathbf{P}			
Leaf Tree	0.1055	0.6048	0.3684	0.0268	
	0.7741	0.0473	0.8630	0.0897	
	0.1204	0.0420	0.5579	0.4001	
Pine (or Needle) Tree	0.3208	0.8532	0.0590	0.0878	
	0.0934	0.5196	0.7269	0.3870	
	0.5195	0.0618	0.1113	0.8269	
Tree Alley	0.8594	0.8845	0.0388	0.0767	
	0.0482	0.6916	0.2816	0.0268	
	0.0925	0.7135	0.0126	0.2739	
Suburban	0.8633	0.9412	0.0808	0.0480	
	0.0197	0.4736	0.2632	0.2632	
	0.1170	0.3540	0.0442	0.6018	
Urban	0.1333	0.7081	0.0436	0.2483	
	0.1531	0.0509	0.9157	0.0334	
	0.7136	0.0436	0.0099	0.9465	

The Pèrez-Fontán model characterizes the satellite channel at different elevation angles, orientations, sides of the road, and environments. In this work, we consider an elevation angle of 30° , the orientation of 45° , and the satellite side of the

Algorithm 1 The D-MBAF algorithm

Input: $\mathcal{C}, \mathcal{B}, \mathcal{T}, \mathcal{D}, R, L$

- 1: $\mathcal{M}_{base} = \emptyset$; \triangleright set of Base MBAs delivering base layers
- 2: $\mathcal{M}_{enh} = \emptyset$; \triangleright set of Enhancement MBAs delivering enhancement layers
- 3: **for** $c \in \mathcal{C}$ **do**
- 4: $\mathcal{B}^* = \emptyset$; \triangleright set of beams transmitting c -th content
- 5: $\mathcal{M} = \emptyset$; \triangleright set of all MBAs delivering c -th content
- 6: **for** $b \in \mathcal{B}$ **do**
- 7: **if** (count NTN terminals interested in c -th content) ≥ 1 **then**
- 8: add b in \mathcal{B}^* ;
- 9: **end if**
- 10: **end for**
- 11: $\mathcal{M} = FindAdjacentBeams(\mathcal{B}^*)$;
- 12: $\mathcal{Q}(\mathcal{T}) = CQIcollection(\mathcal{T})$;
- 13: **procedure** MBA CLASSIFICATION
- 14: **for** $m \in \mathcal{M}$ **do**
- 15: $q_{min} = \min(\mathcal{Q}_m(\mathcal{T}))$; \triangleright minimum CQI experienced by terminals inside the m -th MBA
- 16: $m_b, R_b, ADR_b = CreateBaseMBA(q_{min}, d_{min, b}, m, \mathcal{T})$;
- 17: add m_b in \mathcal{M}_{base} ;
- 18: listCQI = SortUniqueCQI($\mathcal{Q}_m(\mathcal{T})$);
- 19: **if** (listCQI(1) == q_{min}) **then**
- 20: delete listCQI(1) from listCQI;
- 21: **end if**
- 22: **while** $ADR_{c, m}(i) > ADR_{c, m}(i-1)$ **do**
- 23: $R_e = R - R_b$; \triangleright number of available RBs for enhancement MBAs
- 24: $\mathcal{M}_e, \mathcal{R}_e, ADR_e = CreateEnhancementMBA(m, q_{min}, \mathcal{D}_{min, e}, R_e, \mathcal{T}, L, \text{listCQI})$;
- 25: $ADR_{c, m}(i) = ADR_b + ADR_e$;
- 26: **end while**
- 27: **for** $m_e \in \mathcal{M}_e$ **do**
- 28: add m_e in \mathcal{M}_{enh} ;
- 29: **end for**
- 30: **end for**
- 31: **end procedure**
- 32: **end for**
- 33: **return** $ADR = \sum_{c=1}^C \sum_{m=1}^M ADR_{c, m}$

Output: $\mathcal{M}_{base}, \mathcal{M}_{enh}, ADR$.

road. The five environments (i.e. Leaf Tree, Pine (or Needle) Tree, Tree Alley, Suburban, and Urban) are modeled each by a Markov matrix, a state probability vector, and a set of Loo distribution parameters. Table II and Table III show the Loo distribution parameters, the Markov matrix and the probability vector considered in this work.

IV. PROPOSED D-MBAF ALGORITHM

A. Detailed D-MBAF Implementation

Algorithm 1 lists the pseudo-code that describes how the proposed D-MBAF algorithm works.

Table IV reports the main notation used in the pseudo-code.

The algorithm receives as inputs the set \mathcal{C} of content items, the set \mathcal{B} of GEO-sat beams, the set \mathcal{T} of NTN terminals interested in at least one content item, the set \mathcal{D} of minimum

TABLE IV: Notations

\mathcal{C}	set of all eMBB content items requested in the SBA
\mathcal{B}	set of all beams of a GEO-sat
\mathcal{T}	set of NTN terminals requiring broadcast service
\mathcal{L}	set of the Enhancement Video Layers
L	number of Enhancement Video Layers
\mathcal{D}	set of minimum rates required for base and enhancement layers
$d_{min,b}$	minimum rate for the delivery of the base layer
$D_{min,b}$	minimum rate for the delivery of the enhancement layer e
$DR(q_{min})$	data rate associated to the the CQI q_{min}
\mathcal{M}	set of all MBAs
\mathcal{M}_{base}	set of all Base MBAs
\mathcal{M}_{enh}	set of all Enhancement MBAs
\mathcal{M}_e	set of Enhancement MBAs delivering the enhancement layer e
\mathcal{B}^*	set of beams transmitting a content
\mathcal{Q}	set of CQIs experienced by NTN terminals
listCQI	list of CQI supported by the NTN terminals
q_{min}	the CQI influencing the transmission parameters of the base layer
q_e	the CQI influencing the transmission parameters of an enhancement layer
V	vector with a combination of L CQIs influencing the transmission parameters of all the enhancement layers
R	number of available RBs
R_b	number of RBs for offering the minimum rate to the base layer
R_e	number of RBs for delivering enhancement layers
\mathcal{R}_e	set of RBs allocated to each Enhancement MBA
ADR	ADR of the multi-beam NTN system

data rate required for the delivery of the base and enhancement layers, the number R of available radio resources, and the number L of enhancement video layers to deliver (line 1, Algorithm 1). The first step is to check if each beam b belonging to \mathcal{B} contains at least one NTN terminal interested in the content item c in order to add the b -th beam into a supplementary set \mathcal{B}^* of beams (line 3–10, Algorithm 1) representing the input of function *FindAdjacentBeams* (pseudo-code listed in Algorithm 2), which gives at the output the set \mathcal{M} of MBAs wherein the beams satisfy the constraint of adjacency (line 11, Algorithm 1 and lines 1–5, Algorithm 2).

Algorithm 2 Function *FindAdjacentBeams*()

Input: \mathcal{B}^*

- 1: **for** $b_1, b_2 \in \mathcal{B}^*$ **do**
 - 2: **if** AreAdjacent(b_1, b_2)==True **then**
 - 3: add b_1, b_2 in \mathcal{M} ;
 - 4: **end if**
 - 5: **end for**
 - 6: **return** \mathcal{M} .
-

Algorithm 3 Function *CreateBaseMBA*()

Input: $q_{min}, d_{min,b}, m, \mathcal{T}$

- 1: **for** $b \in m$ **do**
 - 2: add b in m_b ;
 - 3: **end for**
 - 4: $R_b = \left\lceil \frac{d_{min,b}}{DR(q_{min})} \right\rceil$;
 - 5: $ADR_b = DR(q_{min}) \times R_b \times |\mathcal{T}|$;
 - 6: **return** m_b, R_b, ADR_b .
-

Algorithm 4 Function *CreateEnhancementMBA*()

Input: $m, q_{min}, D_{min,e}, R_e, \mathcal{T}, L, \text{listCQI}$

- 1: $ADR_e = 0$;
 - 2: Create a vector V of a combination of L CQIs $\in \text{listCQI}$;
 - 3: **for** $l = 1 \rightarrow V$ **do**
 - 4: $q_e = \text{listCQI}(l)$;
 - 5: $T_e = \text{count NTN terminals supporting the CQI } q_e$;
 - 6: **for** $b \in m$ **do**
 - 7: **if** (in the beam b , there are NTN terminals supporting the CQI q_e) **then**
 - 8: add b in m_e ;
 - 9: **end if**
 - 10: **end for**
 - 11: $\mathcal{M}_e = \text{FindAdjacentBeams}(m_e)$;
 - 12: $R_e(l) = \left\lceil \frac{D_{min,b}}{DR(q_e)} \right\rceil$;
 - 13: add $R_e(l)$ in \mathcal{R}_e ;
 - 14: $ADR_e = ADR_e + (DR(q_e) \times R_e(l) \times T_e)$;
 - 15: **end for**
 - 16: **return** $\mathcal{M}_e, \mathcal{R}_e, ADR_e$.
-

After gathering the information on the channel quality (i.e., set \mathcal{Q} of CQIs) of NTN terminals (line 12, Algorithm 1), the algorithm executes the MBA CLASSIFICATION (lines 13–31, Algorithm 1) where, for each MBA m belonging to \mathcal{M} (lines 14–30, Algorithm 1), the base video layer is delivered by adopting the most robust modulation, supported by NTN terminals, driven by the selection of the minimum CQI (q_{min}), and following the CQI-MCS mapping shown in Table V.

TABLE V: CQI-MCS mapping.

CQI index	Modulation Scheme	Spectral Efficiency [bit/s/Hz]	Minimum Rate [kbps]
1	QPSK	0.1523	25.59
2	QPSK	0.2344	39.38
3	QPSK	0.3770	63.34
4	QPSK	0.6016	101.07
5	QPSK	0.8770	147.34
6	QPSK	1.1758	197.53
7	16-QAM	1.4766	248.07
8	16-QAM	1.9141	321.57
9	16-QAM	2.4063	404.26
10	64-QAM	2.7305	458.72
11	64-QAM	3.3223	558.72
12	64-QAM	3.9023	655.59
13	64-QAM	4.5234	759.93
14	64-QAM	5.1152	859.35
15	64-QAM	5.5547	933.19

The pseudo-code for the function *CreateBaseMBA*() is listed in Algorithm 3, where each beam b belonging to each MBA m delivers the base video layer (lines 1–3, Algorithm 3) by exploiting R_b radio resources necessary to achieve the minimum rate indispensable to guarantee the base video resolution (line 4, Algorithm 3). Then, the contribution of ADR for the base video layer delivery is computed (line 5, Algorithm 3).

Once the set \mathcal{M}_{base} of the *Base MBAs* delivering the content with a base resolution by employing R_b radio resources is defined, the algorithm proceeds by sorting in ascending order the CQIs experienced by NTN terminals and leaving all CQIs greater than the lower CQI that will influence the transmission

parameters for the enhancement video layer delivery (lines 18–21, Algorithm 1). The next step is to identify the *Enhancement MBAs* where shared beams shall broadcast the content with higher video resolutions over the remaining radio resources (i.e., \mathcal{R}_e).

The function *CreateEnhancementMBA*, listed in Algorithm 4, defines a combination of as many CQIs as the enhancement video layers to be delivered (line 2, Algorithm 4) and, for each of them, selects the beams where there are NTN terminals supporting that CQI, in order to create an Enhancement MBA after satisfying the constraint of beam adjacency (lines 3–11, Algorithm 4). The function *CreateEnhancementMBA* is also responsible for the efficient radio resource allocation among Enhancement MBAs in order to offer the minimum rate required for the delivery of each video layer with enhanced resolution and avoid interference among the beams of different MBAs (i.e., inter-MBA interference) (line 12–13, Algorithm 4). Then, the contribution of ADR for the enhancement video layer delivery is computed (line 14, Algorithm 4). This step is repeated until the combination of Enhancement MBAs that maximize ADR is found (lines 22–26, Algorithm 1). When the condition of ADR maximization is met, the created Enhancement MBAs are added into the final set \mathcal{M}_{enh} thus improving the video experiences of NTN terminals with better channel conditions (lines 27–30, Algorithm 1). The algorithm proceeds by computing the overall ADR as the sum of data rates experienced by the NTN terminals belonging to Base and Enhancement MBAs (line 33, Algorithm 1). Finally, the algorithm provides at the output the set \mathcal{M}_{base} of Base MBAs, the set \mathcal{M}_{enh} of Enhancement MBAs, and the system *ADR*.

Below, a sample illustration helps to understand how the algorithm works.

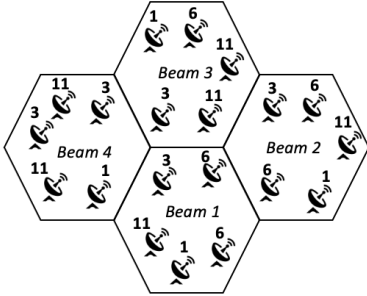


Fig. 3: Illustration of a sample system model.

We consider a simple system with 4 beams and 264 RBs (i.e., 200 MHz), and the CQIs measured by each NTN terminal in each beam as reported in Fig. 3.

The execution of the D-MBAF algorithm will result in the formation of three MBAs, one delivering the base layer and the other two delivering the first and the second enhancement layers, respectively. Specifically, the base MBA delivers the base layer with HD resolution by exploiting 59 RBs and adopting an MCS equal to 1; an enhancement MBA delivers the first enhancement layer with FHD resolution by exploiting 48 RBs and adopting an MCS equal to 3; and an enhancement MBA delivers the second enhancement layer with 4K resolution by exploiting 76 RBs and adopting an MCS equal to 6. It is

worth noting that the number of enhancement MBAs that can be activated depends on the data rate associated to the layer delivered by each of them with a specific video resolution. To deliver the third enhancement layer with 8K resolution, the algorithm would adopt the MCS equal to 11 but, to guarantee the minimum data rate to ensure the 8K video resolution, the system needs 153 RBs against the remaining 81 RBs. Therefore, the algorithm stops and the remaining 81 RBs may be intended for delivering other types of service.

B. Complexity Analysis

In this subsection, we analyze the computational complexity of D-MBAF, which is detailed as follows:

- $O(|\mathcal{C}|)$ is the complexity of implementing the “for” loop over the demanded contents (lines 3–28, Algorithm 1).
- $O(|\mathcal{B}| \cdot |\mathcal{T}|)$ is the complexity of counting, for all beams, the number of NTN terminals interested in a certain service (lines 6–10, Algorithm 1).
- $O(|\mathcal{B}|^2)$ is the complexity of grouping beams into the same MBA while meeting the constraint of beam adjacency (line 11, Algorithm 1).
- $O(|\mathcal{T}|)$ is the complexity of filling a vector, whose length is equal to the number of NTN terminals, with CQI feedbacks (line 12, Algorithm 1).
- $O(|\mathcal{M}|)$ is the complexity of implementing the “for” loop over the MBAs (lines 14–26, Algorithm 1).
- $O(|\mathcal{T}|)$ is the complexity of finding the minimum CQI value among those experienced by the NTN terminals (line 15, Algorithm 1).
- $O(1)$ is the complexity of doing the calculation of both the number of RBs intended for the Base MBA m_b and the achieved ADR (line 16, Algorithm 1).
- $O(|\mathcal{B}|)$ is the complexity of inserting the beams into the final set of Base MBAs (line 17, Algorithm 1).
- $O(|\mathcal{T}|^2)$ is the complexity of sorting in ascending order the CQI values experienced by the NTN terminals (line 18, Algorithm 1).
- $O(1)$ is the complexity of removing the first CQI from the list of experienced CQIs (lines 19–21, Algorithm 1).
- $O(|\mathcal{M}|)$ is the complexity of creating all the Enhancement MBAs and computing both the number of radio resources and ADR (lines 22–26, Algorithm 1). The “while” loop is repeated at most 15 times since the highest CQI value is 15.
- $O(|\mathcal{M}|)$ is the complexity due to the insertion of all the Enhancement MBAs, wherein a given content is delivered with higher video resolution, into the final set of MBAs (lines 27–29, Algorithm 1).
- $O(1)$ is the complexity of computing the overall system ADR (line 33, Algorithm 1).

The implementation of the D-MBAF algorithm has the following polynomial complexity:

$$O(|\mathcal{C}| \cdot (|\mathcal{B}|^2 + |\mathcal{M}|^2 + |\mathcal{B}| \cdot |\mathcal{M}| + |\mathcal{M}| \cdot |\mathcal{T}| + |\mathcal{B}| \cdot |\mathcal{T}| + |\mathcal{T}|^2)).$$

The D-MBAF complexity is reasonable for realistic multi-beam NTN scenarios. Indeed, the execution runtime of the proposed algorithm is feasible thanks to the high-performing gNB, thus making the D-MBAF algorithm compatible with future generation NTN systems.

V. PERFORMANCE EVALUATION

A. Simulation Model

An in-house simulator has been developed based on MATLAB to assess, through a wide simulation campaign, the performance of a 6G multi-beam NTN system when applying the proposed D-MBAF algorithm. The simulator has been calibrated according to the guidelines specified by 3GPP in [1]. Each simulation has been repeated several times to achieve a confidence interval of 95%.

D-MBAF is based on multi-beam transmissions over a single frequency and includes two-way communications. We assume that the NTN terminals demand only one High-Efficiency Video Coding (HEVC)-encoded content, which is delivered in four video flows: a base layer with a minimum data rate of 1.5 Mbps for HD video resolution, the first enhancement layer with a minimum data rate of 3 Mbps for FHD video resolution, the second enhancement layer with a minimum data rate of 15 Mbps for 4K video resolution, and the third enhancement layer with a minimum data rate of 85 Mbps for 8K video resolution [32]. Radio resources are split among the Base and Enhancement MBAs in such a way as to guarantee the minimum required data rate for each layer and to avoid inter-beam interference.

We consider 1000 ms of simulation time corresponding to 100 frames. We uniformly distribute Very Small Aperture Terminals (VSAT) in $\mathcal{B} = 19$ beams. Further modeling parameters are listed in Table VI.

For the five environments under analysis, i.e., Leaf Tree, Pine (or Needle) Tree, Tree Alley, Suburban, and Urban, we assess the performance in two different modeling cases:

- **Case A**, where the number of NTN terminals in the system varies from 500 to 1000 and the channel bandwidth is fixed to 200 MHz¹ (i.e., 264 RBs [33]);
- **Case B**, where the number of NTN terminals per beam is set to 350 and the channel bandwidth varies from 50 to 200 MHz (that corresponds to 66, 132, 264 RBs [33]);
- **Case C**, where the number of NTN terminals in the system is set to 1000 and the channel bandwidth is fixed to 200 MHz (i.e.m 264 RBs [33]).

The proposed D-MBAF algorithm has been compared against multi-layer video delivery over multi-beam NTN system based on a full frequency reuse scheme (i.e., ML-VD (FRF=1)), multi-layer video delivery over multi-beam NTN system based on a four-color frequency reuse scheme (i.e., ML-VD (FRF=2)), multi-layer video delivery over multi-beam NTN system based on a three-color frequency reuse scheme (i.e., ML-VD (FRF=3)), and SF-MBT scheme [5] by evaluating the following performance metrics:

¹The maximum bandwidth allowed per beam is 200 MHz for Ka-band with numerology $\mu = 2$ [1]

TABLE VI: Main Modeling Parameters [1], [2].

PARAMETER	VALUE
NTN architecture option	GEO satellite equipped with transparent payload
GEO altitude	35786 km
GEO EIRP density	40 dBW/MHz
GEO Tx max gain	58.5 dBi
Beam footprint size	110 km (diameter)
Beam footprint type	Fixed
Beam footprint layout	Hexagonal
Number of beams	19
NTN terminal type	VSAT
NTN terminal distribution	100% outdoor
NTN terminal speed	0 kmph
NTN terminal antenna configuration	Directional with 60 cm equivalent aperture diameter
Polarization	Circular
NTN terminal antenna gain	39.7 dBi
NTN terminal noise figure	1.2 dB
NTN terminal Tx power	33 dBm
Carrier frequency	Ka-band (i.e., 20 GHz)
Numerology μ	2
Max bandwidth per beam	200 MHz for Ka-band with $\mu=2$
Sub-carrier spacing	60 kHz
Time slot	0.25 ms
Free space pathloss	$L = 32.45 + 20 \log_{10}(f_c) + 20 \log_{10}(d)$ where: f_c is the carrier frequency; d is the distance between the GEO and the NTN terminal

- **Mean throughput** represents the average data rate achieved by the NTN terminals.
- **ADR** is the sum of all the data rates of the NTN terminals.
- **RB utilization** is the percentage of RBs exploited to deliver all four video flows.
- **Number of sent layers** captures how many video layers are sent and correctly delivered.

B. Analysis of Results

The performance metrics of interest are assessed according to the parameters given as inputs in the cases A, B, and C. The curve for the proposed D-MBAF algorithm has been marked by a dashed line with “◇”, the curve for the ML-VD (FRF=1) scheme by a solid line with “*”, the curve for the ML-VD (FRF=2) scheme by a solid line with “+”, the curve for the ML-VD (FRF=3) scheme by a dash-dotted line with “□”, and the curve for the SF-MBT algorithm by a solid line with “★”.

1) *Case A*: Figs. 4 and 5 illustrate the mean throughput and the ADR, respectively, for the five schemes under analysis for a varying number of NTN terminals in the system. As it can be noted, in all five environments the proposed D-MBAF algorithm achieves better results in terms of mean throughput and ADR than the ML-VD (FRF=2 and FRF=3) and the SF-MBT schemes, but lower results than the ML-VD (FRF=1). However, the ML-VD (FRF=1) results do not consider the effects of interference on NTN terminals deployed at beam edges and receiving the content from signals belonging to different beams and that are not synchronized in time to be combined as constructive sources. This mechanism of combining more signals following different paths and arriving within a certain time interval, instead, happens for the D-MBAF algorithm owing to the introduction of MBSFN Beam transmissions.

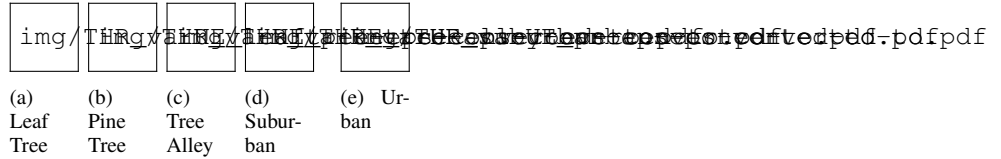


Fig. 4: Mean Throughput for D-MBAF, ML-VD (FRF=1), ML-VD (FRF=2), ML-VD (FRF=3), and SF-MBT with a varying number of NTN terminals.

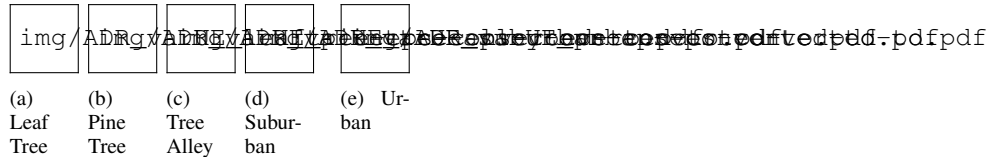


Fig. 5: ADR for D-MBAF, ML-VD (FRF=1), ML-VD (FRF=2), ML-VD (FRF=3), and SF-MBT with a varying number of NTN terminals.

Specifically, as shown in Fig. 4, the mean throughput of D-MBAF follows a near-constant trend in four environments (i.e., 5.5 Gbps in Pine Tree, 11 Gbps in Tree Alley and Suburban, and 2.2 Gbps in Urban) and a slightly decreasing trend in the Leaf Tree environment (i.e., decreasing from about 8 Gbps to just over 6 Gbps, when increasing the number of NTN terminals from 500 to 1000). Increasing the number of NTN terminals boosts the probability to find even a single NTN terminal that experiences adverse channel conditions, thus affecting the choice of group-based transmission parameters (i.e., more robust modulation) and, hence, the throughput of the other NTN terminals in the same MBA. Meanwhile, since the ADR computation is given by the sum of the data rates of all NTN terminals, the curve of the ADR follows a growing trend when increasing the number of NTN terminals in the system in all environments. The highest ADR achieved by the proposed D-MBAF ranges from 5800 to 11000 Gbps in the Tree Alley and Suburban environments, whereas it ranges from 4000 to 6100 Gbps in the Leaf Tree, from 2300 to 5100 Gbps in the Pine Tree, and from 1100 to 2100 Gbps in the Urban environment. It is worth noticing that D-MBAF achieves such high values since, differently from the SF-MBT scheme where each MBA delivers a content with the most robust modulation supported by all NTN terminals, the MBAs of the D-MBAF algorithm are formed by grouping the NTN terminals according to the channel similarity, i.e., using the multicast subgrouping approach. Hence, the beams belonging to each MBA can perform the MBSFN Beam transmission

for the delivery of enhancement video layers with less robust modulation and, in addition, over equal resources such as ML-VD with FRF=1 and more radio resources than ML-VD with FRF=2 and FRF=3. Instead, these two latter schemes overcome the SF-MBT algorithm by benefiting from the advantages of the multi-layer transmission even if the frequency is reused among the beams and fewer radio resources are available in comparison to the proposed D-MBAF algorithm.

2) *Case B*: Figs. 6 and 7 illustrate the mean throughput and the ADR, respectively, for the five schemes under analysis when considering a varying channel bandwidth, from 50 to 200 MHz. In all the considered environments, D-MBAF achieves the highest values of the two metrics of interest with respect to the ML-VD (FRF=2 and FRF=3) and the SF-MBT schemes. Both mean throughput and ADR follow a growing trend for the five schemes since more radio resources are available when an increased channel bandwidth is considered. In detail, for the proposed D-MBAF algorithm, the mean throughput ranges from 0.2 to 5.8 Gbps in the Leaf Tree, 0.2 to 5 Gbps in the Pine Tree, 0.2 to 11 Gbps in the Tree Alley and Suburban, and 0.2 to 2.2 Gbps in the Urban environment. The ADR results achieved by D-MBAF range from 1000 to 39000 Gbps in the Leaf Tree, from 1000 to 35000 Gbps in the Pine Tree, from 1000 to 73000 Gbps in the Tree Alley and Suburban, and from 1000 to 18000 Gbps in the Urban environment. Instead, the other three schemes reach lower mean throughput and ADR than the D-MBAF algorithm, since ML-VD (FRF=2 and FRF=3) schemes perform a multi-layer transmission in each beam over

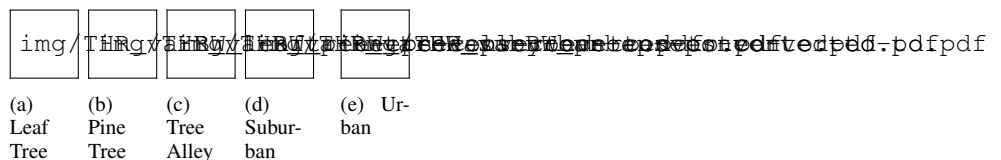


Fig. 6: Mean Throughput for D-MBAF, ML-VD (FRF=1), ML-VD (FRF=2), ML-VD (FRF=3), and SF-MBT with a varying channel bandwidth.

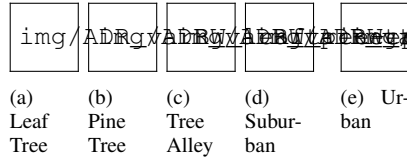


Fig. 7: ADR for D-MBAF, ML-VD (FRF=1), ML-VD (FRF=2), ML-VD (FRF=3), and SF-MBT with a varying channel bandwidth.

fewer radio resources, whereas the SF-MBT scheme selects the most robust modulation to allow all the NTN terminals to decode the delivered content by ensuring fairness at the expense of throughput. As for Case A, the results in terms of mean throughput and ADR achieved by D-MBAF are lower than the ML-VD (FRF=1) due to the fact that the results do not consider that, being able to detect signals coming from different beams, the NTN terminals at beam edges are affected from inter-beam interference. Furthermore, differently from the D-MBAF algorithm where the transmission parameters are chosen on a system basis, the ML-VD (FRF=1) chooses them on a beam basis thus reducing the probability of finding even a single NTN terminal with extremely poor channel conditions as to affect the transmission performance for all the other NTN terminals. Besides achieving the best system-level performance results, the proposed D-MBAF exploits fewer radio resources to deliver more video layers than ML-VD (FRF=2 and FRF=3) and SF-MBT schemes. The fact that D-MBAF uses more radio resources than ML-VD (FRF=1) may depend on the presence of even a single NTN terminal with poor channel conditions that affects the performance of the entire system by lowering the transmission rate thus requiring a greater number of resources. Despite this, D-MBAF is developed to efficiently exploit the radio spectrum thus optimizing the number of radio resources used to provide a given video flow at a certain resolution with the minimum data rate required. The remaining radio resources are left for giving access to other demanded services. Furthermore, the D-MBAF algorithm guarantees the good trade-off in terms of resource utilization and delivered video flows between the ML-VD (FRF=1) and ML-VD (FRF=1 and FRF=2), with the advantage that MBSFN Beam transmissions exploit the constructive interference to enhance the signal received from the NTN terminals in the beam edges, thus eliminating the problem of destructive interference due to schemes based on the full frequency reuse. Indeed, as depicted in Figs. 8 and 9, the D-MBAF algorithm exploits a number of radio resources needed to deliver a certain number of video layers. In particular, when considering a channel bandwidth of 50 MHz, two video layers (i.e., base layer with HD video resolution and first enhancement layer with FHD video resolution) can

img/usage_varBW-eps-converted-to.pdf

Fig. 8: Percentage of RBs exploited by D-MBAF, ML-VD (FRF=1), ML-VD (FRF=2), ML-VD (FRF=3), and SF-MBT with a varying channel bandwidth.

img/sentlayer_varBW-eps-conver

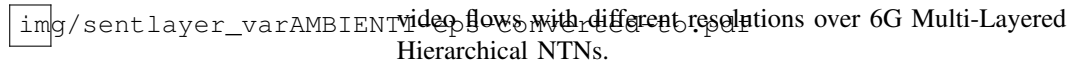
Fig. 9: Number of video layers sent by D-MBAF, ML-VD (FRF=1), ML-VD (FRF=2), ML-VD (FRF=3), and SF-MBT with a varying channel bandwidth.

be delivered by D-MBAF and ML-VD (FRF=1) that uses 30% and 8% of the available radio resources, respectively, against the SF-MBT, ML-VD (FRF=2), and ML-VD (FRF=3) schemes, which deliver only one layer by exploiting 100%, 75%, and 66% of RBs, respectively. For a channel bandwidth of 100 MHz, D-MBAF and ML-VD (FRF=1) can deliver three video layers (i.e., base layer with HD video resolution, first enhancement layer with FHD video resolution, and second enhancement layer with 4K video resolution) by exploiting 38% and 48% of the available radio resources, respectively, against the SF-MBT, which delivers only the base layer over 100% of RBs, whereas ML-VD (FRF=2), and ML-VD (FRF=3) schemes can deliver two video layers (i.e., base layer with HD video resolution and first enhancement layer with FHD video resolution) over 90% and 82% of the available RBs, respectively. Differently from the cases where the channel bandwidth is 50 MHz and 100 MHz and the remaining unused radio resources are not enough to deliver further enhancements, for a channel bandwidth of 200 MHz D-MBAF and ML-VD (FRF=1) can provide all four video layers (i.e., base layer with HD video resolution, first enhancement layer with FHD video resolution, second enhancement layer with 4K video resolution, and third enhancement layer with 8K video resolution) over 32% and 18% of the available radio resources, respectively, whereas the SF-MBT continues to deliver only the base layer over 100% of RBs, and ML-VD (FRF=2), and ML-VD (FRF=3) schemes can deliver at most two video layers (i.e., base layer with HD video resolution and first enhancement layer with FHD video resolution) by exploiting 76% and 68% of the available RBs, respectively.

img/usage_varAMBIENTI-eps-conver

Fig. 10: Percentage of RBs exploited by D-MBAF, ML-VD (FRF=1), ML-VD (FRF=2), ML-VD (FRF=3), and SF-MBT when considering different environments.

3) *Case C*: Figs. 10 and 11 investigate the potentiality of the proposed D-MBAF algorithm in providing a given video content to the NTN terminals in different environments against the other four schemes, when considering 1000 NTN terminals



video flows with different resolutions over 6G Multi-Layered Hierarchical NTN.

Fig. 11: Number of video layers sent by D-MBAF, ML-VD (FRF=1), ML-VD (FRF=2), ML-VD (FRF=3), and SF-MBT when considering different environments.

and a channel bandwidth of 200 MHz. Regardless of the considered environment, D-MBAF and ML-VD (FRF=1) can deliver the four layers with different video resolution by using on average the 32% and 16% of RBs available in the system, respectively, whereas the SF-MBT scheme delivers only one layer over all available RBs due to its working logic. Instead, on average ML-VD (FRF=3) delivers one layer more than ML-VD (FRF=2) owing to more radio resources available by each beam. However, the percentage of RBs exploited by ML-VD (FRF=3) ranges from the 68% to 84% on the basis of both the considered algorithm and the environment.

VI. CONCLUSIONS

In this paper, we proposed the Dynamic MBSFN Beam Area Formation (D-MBAF) algorithm for multicast service delivery in 6G Multi-Beam Non-Terrestrial Networks (NTN). The proposed D-MBAF algorithm dynamically creates dedicated MBSFN Beam Areas (MBA) by leveraging the multicast subgrouping technique. Through simulative campaigns, we compared the system-level performance of the D-MBAF algorithm against the multi-layer video delivery over a multi-beam NTN system based on full-, four-, and three-color frequency reuse schemes, and the SF-MBT scheme. Obtained results confirm that D-MBAF (i) improves the performance of NTN terminals and (ii) enhances the perceived video quality for NTN terminals experiencing better channel conditions owing to the adoption of the multicast subgrouping approach; (iii) boosts the system-level performance by selecting the best MBA configuration that increases the ADR; (iv) avoids inter-beam interference by an efficient management of radio resources, and (v) provides service to all NTN terminals interested in a given content. The proposed D-MBAF is compatible with any satellite architecture based on both single-beam and multi-beam transmissions. In the former case, any satellite (i.e., GEO, MEO, or LEO) covers its footprint with a single beam and, equally, the D-MBAF algorithm can be applied by forming a single base MBA over the entire satellite footprint and more enhancement MBAs, which may illuminate either the entire satellite coverage area or smaller concentric areas where only NTN terminals supporting the selected transmission parameters can receive the content with higher quality levels. It is worth noticing that radio resource management procedures are essential to avoid inter-MBA interference. The latter case has been treated in the paper. The main difference with the previous one is that more base MBAs and more enhancement MBAs delivering the same video layer can be formed, as long as the adjacency constraint among the beams of the same MBA is satisfied. Furthermore, D-MBAF is compatible with any content at any video resolution to broadcast, by adapting the numerology and operational frequency bands. Future works will extend the idea of delivering manifold

REFERENCES

- [1] 3GPP TR 38.821, "Solutions for NR to support non-terrestrial networks (NTN)," Release 16, May 2021.
- [2] 3GPP TR 38.811, "Study on New Radio (NR) to support non terrestrial networks," Release 15, Sept. 2020.
- [3] Ericsson Mobility Report, June 2021. Available at: <https://www.ericsson.com/4a03c2/assets/local/mobility-report/documents/2021/june-2021-ericsson-mobility-report.pdf>.
- [4] A. Guidotti, A. Vanelli-Coralli, G. Taricco, G. Montorsi, "User Clustering for Multicast Precoding in Multi-Beam Satellite Systems," submitted to: *IEEE Transactions on Wireless Communications*, Jun. 2017. Available at: <https://arxiv.org/pdf/1706.09482.pdf>
- [5] F. Rinaldi, H.-L. Määttä, J. Torsner, S. Pizzi, S. Andreev, A. Iera, Y. Koucheryavy, G. Araniti, "Broadcasting Services Over 5G NR Enabled Multi-Beam Non-Terrestrial Networks," in *IEEE Transactions on Broadcasting*, vol. 67, no. 1, pp. 33-45, March 2021, doi: 10.1109/TBC.2020.2991312.
- [6] A. Sali, H. A. Karim, G. Acar, B. Evans, and G. Giambene, "Multicast Link Adaptation in Reliable Transmission Over Geostationary Satellite Networks," in *Wireless Personal Communications*, 2012.
- [7] G. Aiyetoro, G. Giambene, and F. Takawira, "Link Adaptation in Satellite LTE Networks," in *Journal of Advances in Information Technology*, 2014.
- [8] G. Araniti, M. Condoluci, and A. Petrolino, "Efficient Resource Allocation for Multicast Transmissions in Satellite-LTE Networks," in *IEEE Global Communications Conference (GLOBECOM)*, 2013.
- [9] G. Araniti, I. Bisio, M. De Sanctis, A. Orsino, J. Cosmas, "Multimedia Content Delivery for Emerging 5G-Satellite Networks," in *IEEE Transactions on Broadcasting*, 2016.
- [10] G. Araniti, I. Bisio, M. De Sanctis, F. Rinaldi, A. Sciarrone, "Joint Coding and Multicast Subgrouping over Satellite-eMBMS Networks," in *IEEE Journal on Selected Areas in Communications*, May 2018.
- [11] I. Bisio, F. Lavagetto, G. Luzzati, M. Marchese, "Smartphones apps implementing a heuristic joint coding for video transmissions over mobile networks," in *Mobile Networks and Applications*, Vol. 19, No. 4, pp. 552-562, 2014.
- [12] G. Zheng, S. Chatzinotas, B. Ottersten, "Generic Optimization of Linear Precoding in Multibeam Satellite Systems," in *IEEE Transactions on Wireless Communications*, Apr. 2012.
- [13] M. A. Vázquez, A. Pérez-Neira, D. Christopoulos, S. Chatzinotas, B. Ottersten, P.-D. Arapoglou, A. Ginesi, G. Taricco, "Precoding in Multibeam Satellite Communications: Present and Future Challenges," in *IEEE Wireless Communications*, Dec. 2016.
- [14] D. Christopoulos, S. Chatzinotas, B. Ottersten, "Multicast Multigroup Precoding and User Scheduling for Frame-Based Satellite Communications," in *IEEE Transactions on Wireless Communications*, Apr. 2015.
- [15] W. Wang, A. Liu, Q. Zhang, L. You, X. Gao, G. Zheng, "Robust Multigroup Multicast Transmission for Frame-Based Multi-Beam Satellite Systems," in *IEEE Access*, 2018.
- [16] V. Jorroughi, M. A. Vázquez, A. I. Pérez-Neira, "Generalized Multicast Multibeam Precoding for Satellite Communications," in *IEEE Transactions on Wireless Communications*, 2017.
- [17] A. Guidotti, A. Vanelli-Coralli, "Clustering Strategies for Multicast Precoding in Multi-Beam Satellite Systems," submitted to: *International Journal of Satellite Communications and Networking*, Apr. 2018. Available at: <https://arxiv.org/pdf/1804.03891.pdf>
- [18] A. Guidotti, A. Vanelli-Coralli, "Geographical Scheduling for Multicast Precoding in Multi-Beam Satellite Systems," in *2018 9th Advanced Satellite Multimedia Systems Conference and the 15th Signal Processing for Space Communications Workshop (ASMS/SPSC)*, Sept. 2018.
- [19] K. Nakahira, K. Kobayashi, M. Ueba, "A Resource Allocation Scheme for QoS Provision in Multi-Beam Mobile Satellite Communication Systems," in *2007 IEEE Wireless Communications and Networking Conference*, 2007.
- [20] H. Chaouech, R. Bouallegue, "Channel estimation and detection for multibeam satellite communications," in *2010 IEEE Asia Pacific Conference on Circuits and Systems*, Dec. 2010.
- [21] U. Park, H. W. Kim, D. S. Oh, B.-J. Ku, "A Dynamic Bandwidth Allocation Scheme for a Multi-spot-beam Satellite System," in *ETRI Journal*, Aug. 2012.
- [22] S. Liu, X. Hu, W. Wang, "Deep Reinforcement Learning Based Dynamic Channel Allocation Algorithm in Multibeam Satellite Systems," in *IEEE Access*, Apr. 2018.

- [23] A. Paris, I. Del Portillo, B. Cameron, E. Crawley, "A Genetic Algorithm for Joint Power and Bandwidth Allocation in Multibeam Satellite Systems," in *2019 IEEE Aerospace Conference*, Jun. 2019.
- [24] M. Takahashi, Y. Kawamoto, N. Kato, A. Miura, M. Toyoshima, "Adaptive Power Resource Allocation with Multi-Beam Directivity Control in High-Throughput Satellite Communication Systems," in *IEEE Wireless Communications Letters*, Aug. 2019.
- [25] C. Casetti, C.F. Chiasserini, F. Malandrino, C. Borgiattino, "Area Formation and Content Assignment for LTE Broadcasting," *Computer Networks*, vol. 126, pp. 174–186, Oct. 2017.
- [26] G. Araniti, F. Rinaldi, P. Scopelliti, A. Molinaro, and A. Iera, "A Dynamic MBSFN Area Formation Algorithm for Multicast Service Delivery in 5G NR Networks," in *IEEE Transactions on Wireless Communications*, vol. 19, no. 2, pp. 808–821, Feb. 2020.
- [27] F. Rinaldi, S. Pizzi, A. Orsino, A. Iera, A. Molinaro and G. Araniti, "A Novel Approach for MBSFN Area Formation Aided by D2D Communications for eMBB Service Delivery in 5G NR Systems," in *IEEE Transactions on Vehicular Technology*, vol. 69, no. 2, pp. 2058–2070, Feb. 2020.
- [28] H. Liu and H. Wei, "Towards NR MBMS: A Flexible Partitioning Method for SFN Areas," in *IEEE Transactions on Broadcasting*, vol. 66, no. 2, pp. 416–427, June 2020.
- [29] F. Rinaldi, S. Pizzi, A. Molinaro, A. Iera, and G. Araniti, "Frequency Reuse Techniques for eMBB Services over 5G Multi-Beam Non-Terrestrial Networks," in *IEEE International Symposium on Broadband Multimedia Systems and Broadcasting (BMSB)*, 2020.
- [30] F. P. Fontán, M. Vazquez-Castro, C. E. Cabado, J. P. Garcia and E. Kubista, "Statistical modeling of the LMS channel," in *IEEE Transactions on Vehicular Technology*, vol. 50, no. 6, pp. 1549–1567, Nov. 2001.
- [31] C. Loo, "A statistical model for a land mobile satellite link," in *IEEE Transactions on Vehicular Technology*, vol. 34, no. 3, pp. 12–127, Aug. 1985.
- [32] V. Sze, M. Budagavi, and G. J. Sullivan, "High Efficiency Video Coding (HEVC) - Algorithms and Architectures," *Springer*, Jul. 2014.
- [33] 3GPP TS 38.104, "NR; Base Station (BS) radio transmission and reception," Release 16, May 2021.



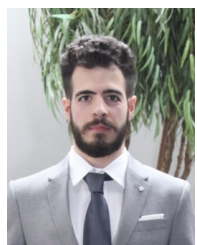
Sara Pizzi is an assistant professor in Telecommunications at University Mediterranea of Reggio Calabria, Italy. From the same University she received the 1st (2002) and 2nd (2005) level Laurea Degree, both cum laude, in Telecommunication Engineering and the Ph.D. degree (2009) in Computer, Biomedical and Telecommunication Engineering. Her current research interests focus on RRM for multicast service delivery, D2D and MTC over 5G/6G networks, integration of NTN in IoT.



Antonella Molinaro graduated in Computer Engineering (1991) at the University of Calabria, received a Master degree in Information Technology from CEFRIEL/Polytechnic of Milano (1992), and a Ph.D. degree in Multimedia Technologies and Communications Systems (1996). She was with Telesoft S.p.A., Rome (1992–1993) and Siemens A.G., Munich, Germany (1994–1995) as a CEC Fellow in the RACE-II program. She was a research fellow at the Polytechnic of Milano (1997–1998), and an assistant professor with the University of Messina (1998–2001) and the University of Calabria (2001–2004). She is currently an associate professor of telecommunications at the University Mediterranea of Reggio Calabria, Italy, and a professor at CentraleSupélec–CNRS–Université Paris-Saclay, France. Her research activity mainly focuses on wireless and mobile networking, vehicular networks, and future Internet.



Federica Rinaldi received the PhD degree in Information Engineering in 2021 from the University Mediterranea of Reggio Calabria, Italy, where she obtained the B.Sc. degree in Telecommunication Engineering and M.Sc. degree (cum laude) in Computer Science and Telecommunication Systems Engineering in 2013 and 2017, respectively. In 2019, she spent six months at Ericsson Research, Finland. Her current research interests include non-terrestrial networks, radio resource management, and multimedia broadcast/multicast service in 5G/B5G networks.



Angelo Tropeano received the M.Sc. degree in Information Engineering from the University Mediterranea of Reggio Calabria, Italy, in 2019, where he is currently pursuing the Ph.D. degree. His area of research includes cellular systems, radio resource management, multicast, and satellite systems.



Giuseppe Araniti received the Laurea degree and the Ph.D. degree in electronic engineering from the University Mediterranea of Reggio Calabria, Italy, in 2000 and 2004, respectively, where he is an Associate Professor of telecommunications. His major area of research is on 5G/6G networks and it includes personal communications, enhanced wireless and satellite systems, traffic and radio resource management, multicast and broadcast services, device-to-device (D2D) and machine-type communications (M2M/MTC).